

# CAPTURE OF SO<sub>2</sub> BY LIMESTONE IN A 71 MW<sub>e</sub> PRESSURIZED FLUIDIZED BED BOILER

by

**Tadaaki SHIMIZU, Mirko PEGLOW, Kazuaki YAMAGIWA,  
Masato TANAKA, Shinichi SAKUNO, Nobuhiro MISAWA,  
Nobuyuki SUZUKI, Hachiro UEDA, Hiroshi SASATSU, and  
Hideki GOTOU**

Original scientific paper  
UDC: 662.613/.62-912  
BIBLID: 0354-9836, 7 (2003), 1, 17-31

*A 71 MW<sub>e</sub> pressurized fluidized bed coal combustor was operated. A wide variety of coals were burnt under fly ash recycle conditions. Limestone was fed to the combustor as bed material as well as sorbent. The emission of SO<sub>2</sub> and limestone attrition rate were measured. A simple mathematical model of SO<sub>2</sub> capture by limestone with intermittent solid attrition was applied to the analysis of the present experimental results. Except for high sulfur fuel, the results of the present model agreed with the experimental results.*

*Key words: pressurized fluidized bed combustor, limestone, sulfur dioxide, attrition, coal*

## Introduction

Pressurized fluidized bed combustors (PFBCs) have been developed as a high efficiency power generation technology. One of the features of PFBCs is *in-situ* SO<sub>2</sub> capture by uncalcined limestone (CaCO<sub>3</sub>). In PFBCs, the partial pressure of CO<sub>2</sub> exceeds the equilibrium partial pressure for calcination (thermal decomposition) of CaCO<sub>3</sub>. Thus the direct reaction between SO<sub>2</sub> and CaCO<sub>3</sub> takes place as follows:



Since the uncalcined limestone is non-porous, the reaction takes place at the external surface of the particle to form a product (CaSO<sub>4</sub>) layer. The rate of reaction has been investigated mainly by use of thermogravimetric analysis [1-7]. The reaction rate was observed to be governed by both chemical kinetics and diffusion of SO<sub>2</sub> through the product layer. The reaction rate constant, order of reaction, and effective diffusivity through the product layer have been evaluated for different types of limestone.

One difference between actual PFBC system and thermogravimetric analysis is attrition of particle. In PFBCs, limestone surface is removed by attrition. Sakuno *et al.* 8 and Shimizu *et al.* 9 evaluated the attrition rate of limestone in a large-scale (71MW electricity output) PFBC and reported that the average attrition rate (reduction rate of radius) was approximately 1-2  $\mu\text{m}/\text{h}$ . The present authors have developed a model of  $\text{SO}_2$  capture by a limestone particle under solid attrition conditions assuming shrinking unreacted core model for reaction 9;  $\text{SO}_2$  reacts with  $\text{CaCO}_3$  only at unreacted core surface and the product layer ( $\text{CaSO}_4$ ) of solid conversion of unity is formed at the surface. If continuous attrition of limestone was assumed, the fine particles removed from the limestone surface consisted of only  $\text{CaSO}_4$  as far as the product layer existed at the surface and  $\text{SO}_2$  capture rate was nearly the same as the solid attrition rate. However, their model was found to overestimate the overall  $\text{SO}_2$  capture rate in the 71  $\text{MW}_e$  PFBC 9; the rate of  $\text{SO}_2$  capture was only 1/3 of the solid attrition rate. Then intermittent attrition model was proposed 10; the external surface layer was removed by attrition intermittently. The overall  $\text{SO}_2$  capture rate under intermittent attrition conditions was found to be lower than the rate under continuous attrition conditions. Thus the overestimation of  $\text{SO}_2$  capture rate could be avoided. A distributed reaction model was also employed instead of shrinking core model 11; the reaction was assumed to take place in a reaction zone near the surface and the conversion of solid at the surface was less than unity. However, such reaction model still overestimated  $\text{SO}_2$  capture when continuous attrition was assumed. When intermittent attrition was assumed, the results of the distributed reaction model were nearly identical to those of the shrinking unreacted core model. Therefore, intermittent nature of attrition was considered to be quite significant. From another viewpoint, the continuous attrition model is not realistic; the fine particles formed by the continuous attrition are infinitely small. The actual fine particles from the combustors must have finite size, thus the attrition is considered to occur intermittently.

Based on the intermittent attrition model assuming the shrinking core model, a simplified PFBC model was proposed 10. The interval of attrition was given as a fitting parameter. By comparing the model results and  $\text{SO}_2$  emission from the 71  $\text{MW}_e$  PFBC during combustion of one kind of coal, the interval of attrition was estimated to be 5 hours.

In the previous study 10, however, the experimental results obtained during combustion of only one kind of coal without fly ash recycle was analyzed by the model. The applicability of the model to different type of coals and different operation conditions has not yet been clarified. In the present work, the intermittent attrition model was applied to the analysis of the experimental results obtained using wide variety of coals under fly ash recycle conditions.

### PFBC experiments

Experiments were conducted using a 71  $\text{MW}_e$  pressurized fluidized bed combustor (fig. 1). The fluidized bed reactor was installed in a pressure vessel. The

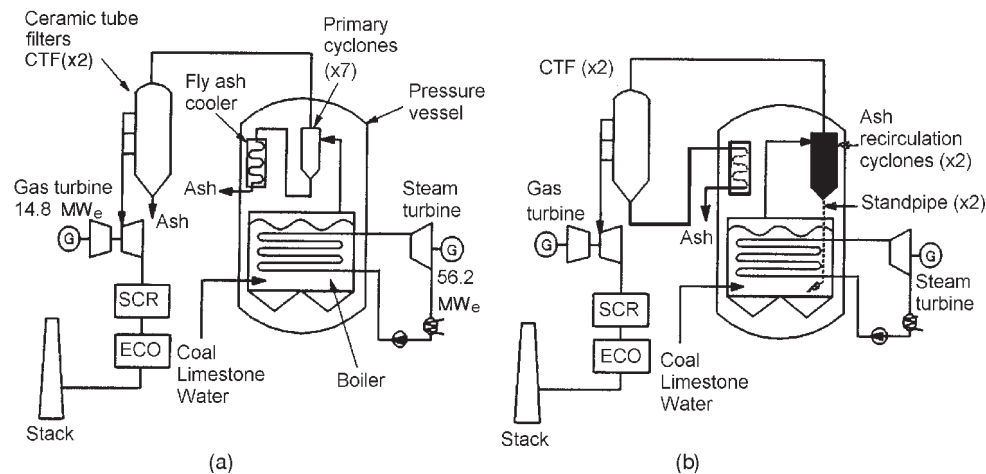


**Figure 1. Schematic diagram of 71 MW<sub>e</sub> PFBC**  
 (a) Phase-1 configuration without ash recycle, (b) Phase-2 configuration with ash recycle

cross section of the reactor was 7 × 4 m and the total height was 8 m. Bed height was varied with load change to control the number of boiler tubes immersed in the dense bed, thus to control the heat recovery rate; the bed height was 3.5 and 2 m at the full load and 50% load, respectively. Total pressure was also varied with load and it was 1.1 and 0.7 MPa at the full load and 50% load, respectively. Temperature in the bed was fixed at 1100–1135 K. The gas velocity was kept constant at 0.9 m/s. The carry-over size of limestone was estimated to be 0.25 mm. The gas residence time in the freeboard was approximately 5–7 s. In the previous study [10], the results obtained without fly ash recycle (Phase-1 configuration in fig. 1) was analyzed during combustion of one kind of coal (BA coal). In the present study the results obtained with fly ash recycle was analyzed (Phase-2 configuration in fig. 1). The fine particles greater than 0.075 mm were captured by cyclones and recycled to the bed. The fly ash smaller than 0.075 mm was captured by ceramic filters after the cyclones and drained from the system. The experimental conditions and SO<sub>2</sub> concentration in the flue gas are summarized in tab.1.

In the present work, four kinds of coal were employed as fuel (tab. 2). The fuel was mixed with water and limestone to form paste and fed to the bottom of the reactor. One kind of limestone was employed as sorbent (tab. 3). The size distribution of limestone is shown in fig. 2. *Ca/S* molar ratios of 2.5–7.7 were adopted for the present study. Such high *Ca/S* ratio was necessary not to achieve SO<sub>2</sub> capture but to maintain the bed height during combustion of low-sulfur coal since the bed material, which mainly consisted of limestone, was lost by attrition; certain bed height is required for heat transfer to the boiler tubes, thus excess limestone feed was required to compensate the loss of limestone. The excess limestone feed resulted in quite low emission of SO<sub>2</sub> (<30 ppm) as shown in tab. 1.

**Table 1. Operation conditions, SO<sub>2</sub> emission and bed material surface area**

Run ID	Coal <sup>a</sup>	Power MWe	Ca/S –	Coal feed rate (dry) kg/s	Limestone feed rate kg/s	Bed material weight 10 <sup>3</sup> kg	O <sub>2</sub> conc. <sup>b</sup> %	SO <sub>2</sub> conc. <sup>b</sup> ppm	Bed material surface area 10 <sup>5</sup> m <sup>2</sup>
1998/11/20	BA	66.0	3.6	6.37	0.218	56.1	6.2	13	2.72
1988/12/16	BA	66.0	3.6	6.06	0.210	54.8	6.6	7	2.19
1999/3/18	BA	35.0	4.8	3.68	0.170	38.2	9.5	3	1.37
1999/4/21	NT	37.0	3	3.56	0.209	37.8	7.5	30	1.35
1999/9/17	BA(7) + AD(3)	57.0	7.7	5.73	0.400	49.6	6.8	16	1.71
1999/10/5	DT	32.5	2.5	3.61	0.294	33.0	9.1	29	1.21
1999/10/11	BA	50.8	4.8	5.03	0.232	44.9	7.2	3	1.71
1999/10/18	BA(5) + DR(5)	36.8	2.5	3.83	0.204	35.3	7.1	21	1.79
1999/10/27	BA(5) + DR(5)	36.5	2.5	0.00	0.207	32.9	7.9	13	1.69

*a* – Coal<sub>1</sub>(p) + Coal<sub>2</sub>(q); coal<sub>1</sub> and coal<sub>2</sub> were mixed with a weight ratio of Coal<sub>1</sub>:Coal<sub>2</sub> = p:q

*b* – Measured at the outlet of gas turbine

**Table 2. Analyses of fuels**

Fuel	Coal			
	BA	NT	AD	DR
F.C. <sup>a</sup> wt.%	58.5	54.0	43.2	51.1
V.M. <sup>b</sup> wt.%	27.0	33.6	44.5	34.1
Ash wt.%	7.8	9.4	1.0	14.1
Moisture wt.%	11.7	7.6	12.8	9.0
Total S wt.%	0.31	0.52	0.10	0.86
HHV kcal/kg	6730	7000	6150	6680

*a* – Fixed carbon, *b* – Volatile matter

**Table 3. Analysis of limestone**

Limestone	CaCO <sub>3</sub>	CaSO <sub>4</sub>	SiO <sub>2</sub>	Al <sub>2</sub> O <sub>3</sub>	Fe <sub>2</sub> O <sub>3</sub>	MgO	CaO
Tsukumi	93.80	0.07	0.10	0.01	0.03	0.49	0.49

## Results of PFBC experiments

In tab. 4, the average attrition rate of limestone,  $\alpha$ , is shown. Attrition rate of limestone within the bed was evaluated from the calcium flux in the fly ash. The drain rate of fly ash and calcium content in the fly ash were measured experimentally. There are three sources of calcium in the fly ash as follows:

(1) calcium from the fine limestone particles (smaller than the cut size of cyclone) in the fed limestone,  $F_{Ca,LF}$ ,

(2) calcium in coal ash which is assumed to be broken into fine particle,  $F_{Ca,CA}$ ,  
and

(3) calcium in the fine limestone particles formed by attrition,  $F_{Ca,AT}$ .

**Table 4. Evaluation of the formation rate of fine limestone particles due to attrition**

Run ID	Fly ash drain rate kg/s	Ca in fly ash %	Feed rate of ash in coal kg/s	Ca in coal ash %	Feed rate of Ca in fine limestone, $F_{Ca,LF}$ mol/s	Feed rate of Ca in coal ash, $F_{Ca,CA}$ mol/s	Ca flow out rate in fly ash, $F_{Ca,FA}$ mol/s	Fine Ca formation rate by attrition, $F_{Ca,AT}$ mol/s
1998/11/20	0.573	10.6	0.592	0.4	0.07	0.06	1.52	1.39
1988/12/16	0.625	13.0	0.548	0.3	0.12	0.04	2.02	1.87
1999/3/18	0.406	12.7	0.345	0.2	0.03	0.02	1.29	1.24
1999/4/21	0.398	13.6	0.383	4.0	0.14	0.39	1.35	0.82
1999/9/17	0.490	13.8	0.669	1.9	0.21	0.32	1.69	1.17
1999/10/5	0.552	11.5	0.498	3.2	0.18	0.40	1.59	1.01
1999/10/11	0.563	11.5	0.392	1.2	0.14	0.12	1.62	1.36
1999/10/18	0.535	14.0	0.335	5.8	0.25	0.49	1.87	1.13
1999/10/27	0.550	15.9	0.335	5.8	0.28	0.49	2.18	1.41

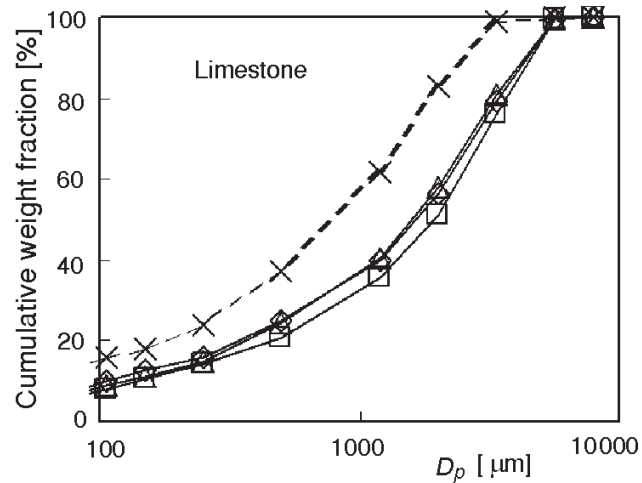
The feed rate of fine limestone particles was calculated from the feed rate of limestone (tab. 1) and size distribution of limestone (fig. 2). Feed rate of calcium in coal ash was calculated from the coal feed rate, ash content in the coal and calcium content in the ash, assuming that all of the ash was broken into small particles and carried over by the flue gas since the ash was fragile. As shown in tab. 4, the contribution of calcium in coal ash to total flux of Ca in the fly ash was only minor, thus the assumption of the behavior of coal ash was not so important. By subtracting  $F_{Ca,LF}$  and  $F_{Ca,CA}$  from total flux of Ca in fly ash ( $F_{Ca,FA}$ ), Ca in the fine particles formed by attrition was obtained as shown in tab. 4 as follows:

$$F_{Ca,AT} = F_{Ca,FA} - F_{Ca,CA} - F_{Ca,LF} \quad (2)$$

From the formation of fine Ca-containing particles due to attrition, average limestone attrition rate (rate of change in radius with time),  $\alpha$ , was obtained as follows:

**Figure 2. Size distribution of limestone fed to the bed**

- 1998/12/16-BA
- ◇ 1999/4/21-NT
- △ 1999/10/05-DR
- × 1999/10/27BA +DR



$$\alpha = \frac{F_{Ca,AT}M}{\rho A} \quad (3)$$

External surface area of the bed material ( $A$ ) was calculated from the total mass of the bed material ( $W_{BM}$ ) and size distribution of the bed material (fig. 3) as follows:

$$A = \frac{6W_{BM}}{\rho} \sum \frac{w_i}{D_{pi}} \quad (4)$$

where  $\rho$ ,  $D_{pi}$ , and  $w_i$  are density of limestone, particle size of bed material of  $i$ -th fraction, and mass fraction of bed material that has size of  $D_{pi}$ , respectively. The mass of the bed material was estimated from the pressure drop across the bed. The amount of the bed material and external surface area of limestone are shown in tab. 1.

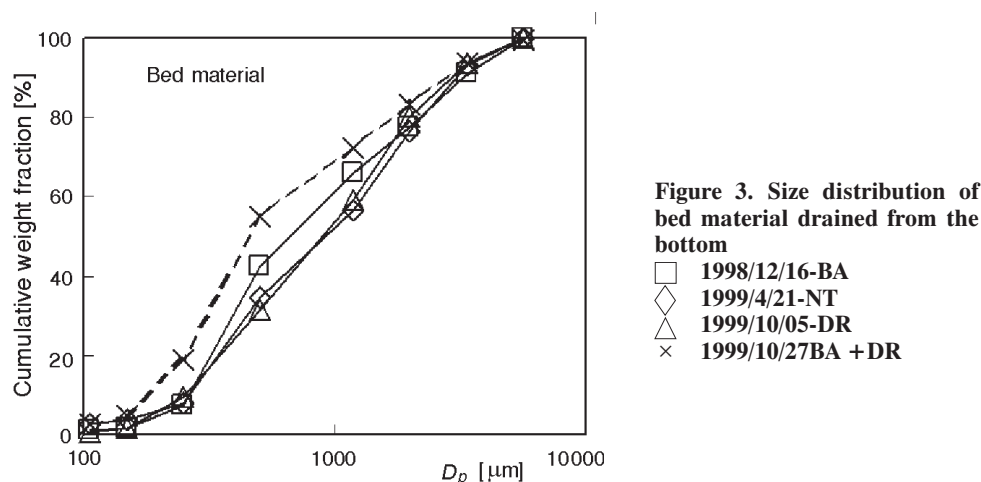


Figure 3. Size distribution of bed material drained from the bottom

- 1998/12/16-BA
- ◇ 1999/4/21-NT
- △ 1999/10/05-DR
- × 1999/10/27BA + DR

Figure 4 shows the relationship between plant power output and attrition rate for various coals. The average attrition rate was approximately 1 m/h and the influence of plant power output on the attrition rate was only minor. This is attributable to the constant gas velocity throughout the operating conditions; the gas velocity was kept constant by changing both air feed rate and total pressure in the vessel. Also the fuel type had little influence on the attrition rate. This indicates that the interaction between the fuel and the limestone was not important.

Concentration of  $SO_2$  in the flue gas was between 3 and 30 ppm (tab. 1). Figure 5 shows the relationship between  $Ca/S$  molar ratio and  $SO_2$  removal efficiency.  $Ca/S$  ratio was calculated from the feed rate of limestone, feed rate of coal and sulfur content in the coal.  $SO_2$  removal efficiency was calculated from the sulfur content of the fuel, coal feed rate, air feed rate and the concentration of  $SO_2$  in the flue gas. Though it is usual that the  $SO_2$  emission is discussed in relation to  $Ca/S$  ratio,  $Ca/S$  ratio was not a good index to describe the sulfur capture behavior in the present PFBC.

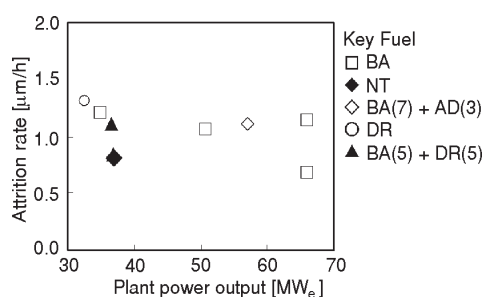


Figure 4. Effect of plant power output and fuel type on attrition rate

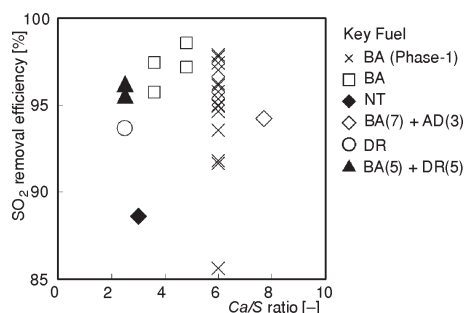


Figure 5. Effect of Ca/S ratio on SO<sub>2</sub> removal efficiency

### A simplified model of SO<sub>2</sub> capture by limestone in PFBC

#### Simple model of SO<sub>2</sub> capture by limestone surface

A modification of shrinking unreacted core model was employed in the present model. At the external surface of a limestone particle, product (CaSO<sub>4</sub>) layer is formed. Reactants (SO<sub>2</sub> and O<sub>2</sub>) diffuse through the product layer and they react with CaCO<sub>3</sub> at the unreacted core surface. Since the concentration of O<sub>2</sub> is far higher than that of SO<sub>2</sub>, only the diffusion of SO<sub>2</sub> is taken into consideration.

In the previous study, the product layer thickness was calculated to be less than 10 µm and this was far smaller than the particle size in the bed, thus flat surface approximation was employed. The reaction system for a flat surface is described schematically in fig. 6.  $X$  is the distance from the initial surface (surface at time = 0) into

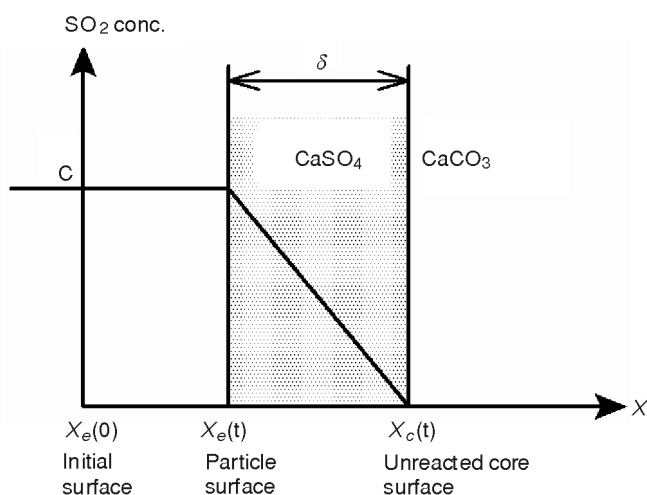


Figure 6. Schematic diagram of SO<sub>2</sub> capture by limestone particle assuming flat surface and "diffusion controlling"

the direction to the particle's center. The position of the center of particle is fixed.  $X_e$  and  $X_c$  denote the positions of external surface and unreacted core surface at time =  $t$ , respectively. Product layer thickness  $\delta$  is:

$$\delta = X_c - X_e \quad (5)$$

In the previous study, the overall reaction rate was found to be mainly governed by the diffusion of  $\text{SO}_2$  through the product layer. Thus the assumption of "diffusion controlling" was employed. The specific reaction rate ( $\text{SO}_2$  capture rate per unit external surface area),  $q_s$ , under diffusion controlling condition is given as follows:

$$q_s = \frac{D_e C}{\delta} \quad (6)$$

where  $D_e$  and  $C$  are the effective diffusivity through the product layer and concentration of  $\text{SO}_2$  at the external surface, respectively. A value of  $D_e = 1.5 \cdot 10^{-9} \text{ m}^2/\text{s}$  was adopted; this value was based on the results of the TGA study by Qui and Lindqvist [7] and modified by Shimizu *et al.* [9] for the application to thin product layer.

The change in the distance between the unreacted core surface and the initial particle surface is given as follows:

$$\frac{dX_c}{dt} = \frac{D_e C M}{\rho \delta} \quad (7)$$

where  $M$  and  $\rho$  are molecular weight of  $\text{CaCO}_3$  and density of limestone, respectively.

The external surface is removed by attrition. Figure 7 illustrates the change in the particle radius with time under intermittent solid attrition conditions. To make the model simple, periodical attrition was assumed. The external surface was removed with an interval of  $\tau$ , thus the change in  $X_e$  was given as follows:

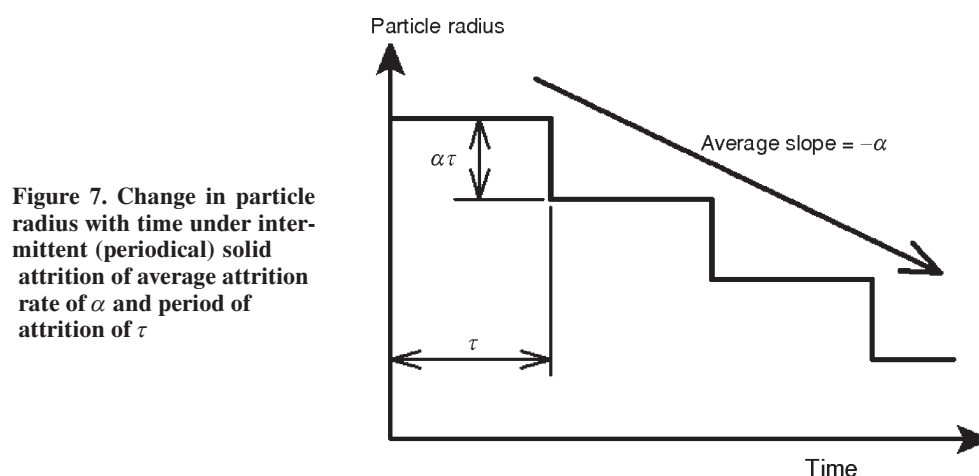


**Figure 7. Change in particle radius with time under intermittent (periodical) solid attrition of average attrition rate of  $\alpha$  and period of attrition of  $\tau$**

$$X_e(t) = X_e(0) + (\alpha\tau)\text{int}(t/\tau) \quad (8)$$

where the function  $\text{int}(t/\tau)$  yields the integer part of  $t/\tau$ .

By assuming intermittent attrition, the change in the product layer thickness, with the exception of the moment of attrition, is given as follows:

$$\frac{d\delta}{dt} = \frac{D_e CM}{\rho\delta} \quad (j\tau < t < (j+1)\tau, \quad j = 0, 1, 2, \dots) \quad (9)$$

If the fresh CaCO<sub>3</sub> surface appears when attrition occurs, the thickness of the product layer at the moment of attrition  $t = j\tau$  ( $j = 0, 1, 2, \dots$ ) is zero. By solving eq. 9, the product layer thickness is given as a function of time as follows:

$$\delta(t) = \frac{2D_e CM(t - j\tau)^{1/2}}{\rho} \quad (j\tau < t < (j+1)\tau, \quad j = 0, 1, 2, \dots) \quad (10)$$

The average rate of increase in the product layer thickness during one period of attrition, from  $t = 0$  to  $t = \tau$ , is given as follows:

$$\left. \frac{d\delta}{dt} \right|_{\text{average}} = \frac{\delta(\tau)}{\tau} = \frac{2D_e CM}{\rho\tau} \quad (11)$$

Thus the average SO<sub>2</sub> capture rate per unit surface area,  $r_s$ , is given as follows:

$$r_s = \frac{\delta(\tau)}{\tau} \frac{\rho}{M} = \frac{2D_e \rho}{M\tau} C^{1/2} \quad (12)$$

The criteria if the fresh CaCO<sub>3</sub> surface appears when intermittent attrition occurs is given as follows:

$$\alpha\tau > \delta(\tau) = \frac{2D_e CM\tau^{1/2}}{\rho} \quad (13)$$

The conversion of CaCO<sub>3</sub> to CaSO<sub>4</sub> in the fragment is given as the ratio of thickness of the product layer to the removed thickness by attrition:

$$\eta = \frac{\delta(\tau)}{\alpha\tau} = \frac{\frac{2D_e CM\tau^{1/2}}{\rho}}{\alpha\tau} \quad (14)$$

In the present work, the fresh CaCO<sub>3</sub> surface was assumed to appear when intermittent attrition occurs since the overall attrition rate was far higher than that of overall SO<sub>2</sub> capture rate. The fragment formed by attrition contained unreacted CaCO<sub>3</sub>, *i. e.*  $\eta < 1$ . Thus  $\alpha\tau$  is considered to be greater than  $\delta(\tau)$  and fresh CaCO<sub>3</sub> appears.

*Model of SO<sub>2</sub> capture by limestone surface in PFBC*

Formation of SO<sub>2</sub> from fuel occurs during volatile matter combustion as well as char combustion. Volatile matter combustion is assumed to take place at the bottom of the bed; Suzuki conducted bench-scale PFBC experiments using a transparent quartz reactor installed in a pressure vessel and found that combustion of volatile matter took place only at the bottom of the reactor [12]. Thus SO<sub>2</sub> concentration at the bottom of the combustor,  $C(0)$ , is given by the rate of SO<sub>2</sub> formation from volatile matter and gas flow rate,  $V_G$ :

$$C(0) = \frac{G_{\text{coal}} s_{\text{coal}} VM_{\text{coal}}}{V_G} \quad (15)$$

where  $G_{\text{coal}}$  and  $s_{\text{coal}}$  are coal feed rate and sulfur content in fuel, respectively.  $VM_{\text{coal}}$  is the portion of sulfur released as volatile matter. In the present study,  $VM_{\text{coal}}$  is assumed to be the same as volatile matter content of fuel.

SO<sub>2</sub> formation from char is assumed to occur uniformly throughout the bed since the solids are considered to be completely mixed in the fluidized bed. The SO<sub>2</sub> evolution rate per unit mass of bed material,  $R_F$ , is given as follows:

$$R_F = \frac{G_{\text{coal}} s_{\text{coal}} FC_{\text{coal}}}{W_{BM}} \quad (16)$$

where  $FC_{\text{coal}}$  is fixed carbon content of coal.

The bed material is assumed to consist of only limestone since the coal ash is so fragile that it is broken into fine particle and carried by the flue gas stream. Indeed, we obtained coal ash sample by burning coal in air at 1088 K and found that the ash was so fragile that it could be easily crushed by finger. In contrast, uncalcined limestone was hard even after treating at 1123 K in pure CO<sub>2</sub> stream. Thus it is very unlikely that the ash resided in the bed for long time.

The rate of SO<sub>2</sub> capture per unit mass of bed material,  $R_S$ , is given from the SO<sub>2</sub> capture rate per unit surface area of limestone, total surface area of limestone in the bed and total mass of bed material as follows:

$$R_S = \frac{r_s A}{W_{BM}} = \frac{A}{W_{BM}} \frac{2D_e \rho}{M\tau} C^{1/2} \quad (17)$$

In the 71MW<sub>e</sub> PFBC, the particle size in the bed was mainly 0.25-5 mm (fig. 3). For fluidized beds consists of such coarse particles, in which gas velocity is higher than bubble rising velocity, mass transfer resistance between bubble and emulsion is not so important, thus the bed can be treated as a plug-flow reactor [13]. In such reactor, the change in SO<sub>2</sub> concentration with contact with solids is given as follows:

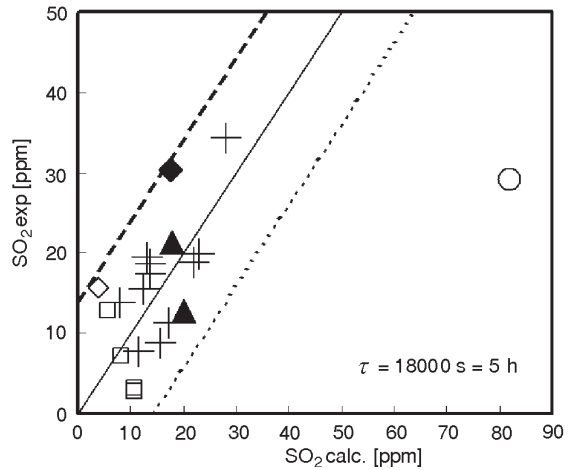
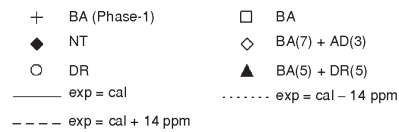
$$\frac{V_G dC}{dW_{BM}} = R_F - R_S \quad (18)$$

By solving this equation numerically with initial value  $C(0)$  from eq. 15, the concentration profile along the bed height as well as flue gas SO<sub>2</sub> concentration were obtained.

### Comparison of SO<sub>2</sub> emission between model and experiments

Figure 8 shows the comparison between experimental value of SO<sub>2</sub> emission and results of model calculation giving  $\tau$  as a parameter. In the previous study 10, the experimental value agreed fairly well with the experimental value when  $\tau$  was assumed to be 5 hours (=18000 s) for BA coal combustion without fly ash recycle. In the present study, the same value of  $\tau$  was assumed. For most of the results of the present study, with fly ash recycle and for different type of coals, the data fall within an area of error of 14 ppm. This error is considered to be sufficiently small for the practical use. Though the present model was developed based on PFBC results without fly ash recycle, the present model is applicable to PFBC with fly ash recycle.

**Figure 8. Comparison between experimentally obtained SO<sub>2</sub> emission and calculated SO<sub>2</sub> emission assuming  $\tau$  of 5 hours (results of BA coal combustion without fly ash recycle 10 are denoted with +)**



For only DR coal, the deviation between the model and the experimental result was remarkable. This deviation is attributable to the limitation of the present simple reaction model. The present model assumes that the fresh CaCO<sub>3</sub> is exposed when attrition occurs (eq. 13). This condition is rewritten in terms of solid utilization as follows:

$$\eta \frac{\delta(\tau)}{\alpha\tau} = 1 \quad (19)$$

Due to the high sulfur content, the condition in the reactor for DR coal is close to the limit. As shown in fig. 9, the total SO<sub>2</sub> capture rate per total attrition rate for DR

coal was the highest among fuels tested. Total SO<sub>2</sub> capture rate within the reactor (Y) was given from the feed rate of S in the coal and the flux of SO<sub>2</sub> in the flue gas as follows:

$$Y = G_{\text{coal}} S_{\text{coal}} - V_G C_{\text{exit}} \quad (20)$$

where  $C_{\text{exit}}$  is the concentration of SO<sub>2</sub> at the exit of the reactor.

$$\eta_{\text{exper}} = \frac{Y}{F_{\text{Ca,AT}}} \quad (21)$$

For DR coal, the value of  $\eta_{\text{exper}}$  was nearly 0.8 and those for others were less than 0.6. Though in the present model only single value of  $\tau$  was assumed, it is conceivable that  $\tau$  has distribution. When the experimental condition is close to the limit given as eq. 13 or eq. 19, some limestone particles may exceed the limit if  $\tau$  has distribution. When the utilization is sufficiently smaller than unity, all the particles fall in the limit even if  $\tau$  has distribution.

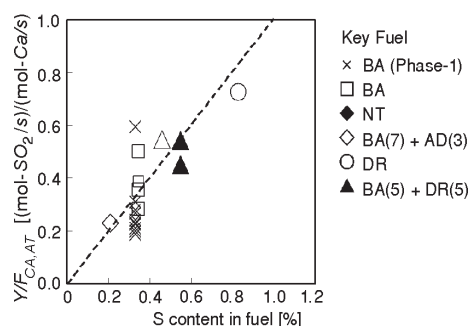


Figure 9. Effect of sulfur content of fuel on the ratio of total SO<sub>2</sub> capture rate in PFBC and overall limestone attrition rate

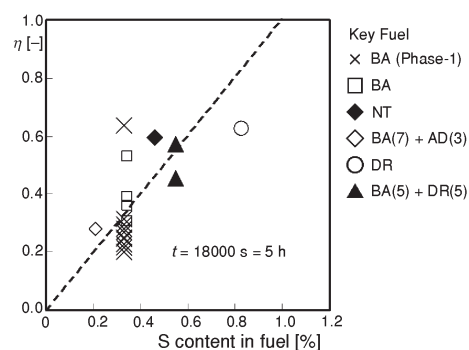


Figure 10. Effect of sulfur content of fuel on the utilization of limestone (theoretical results)

Figure 10 shows the relation between sulfur content of fuel and limestone utilization efficiency calculated theoretically according to eq. 14. Similar relationship between sulfur content and limestone utilization efficiency to fig. 9 was obtained. The present model was effective not only estimation of SO<sub>2</sub> emission but also limestone utilization efficiency.

As discussed above, the attrition interval ( $\tau$ ) plays an important role in determining desulfurization behavior of limestone. However, the period of attrition in PFBCs has not yet been evaluated. The attrition interval can be evaluated if the size distribution of limestone fines formed by attrition is obtained; the size of limestone fragment is considered to be approximately  $\alpha\tau$ . However, the fly ash includes both limestone fines and coal ash, thus only the Carich particles should be picked up and the size of such particles should be measured. For such purpose, CC-SEM (Computer-Controlled-SEM) may give useful information. However, the size distribution data is not yet available at this moment. This is a subject of future works.

## Conclusion

A wide variety of coals were burnt in a 71 MW<sub>e</sub> pressurized fluidized bed combustor under fly ash recycle conditions. The emission of SO<sub>2</sub> was between 3 to 30 ppm. SO<sub>2</sub> removal efficiency was not correlated with Ca/S ratio. Attrition rate of limestone was evaluated from the drain rate of calcium in fly ash. Limestone attrition rate was approximately 1 μm/h and it was not affected by the coal type and plant power output. The ratio of total sulfur capture rate to limestone attrition rate was nearly proportional to the sulfur content of fuel.

A simplified model of SO<sub>2</sub> capture by limestone under pressurized fluidized bed combustion conditions was applied to the analysis of the present PFBC. In this model, intermittent attrition of limestone was assumed. By giving a value of the period of attrition of 5 hours, which was obtained in the previous work without fly ash recycle, the experimental results agreed well with the model for most of the coal, except for high sulfur content coal.

## Acknowledgement

T. Shimizu thanks The Ministry of Education, Culture, Sports, Science, and Technology for Grant-in-Aids (No.11218204). The authors express their thanks to The Ministry of International Trade and Industry, Agency of Natural Resources and Energy, and Center for Coal Utilization, Japan, for the financial aid for 71 MW<sub>e</sub> PFBC test project.

## Nomenclature

$A$	– external surface area of bed material, m <sup>2</sup>
$C$	– SO <sub>2</sub> concentration in gas, kmol/m <sup>3</sup>
$C_{\text{exit}}$	– SO <sub>2</sub> concentration at the exit of reactor, kmol/m <sup>3</sup>
$D_{pi}$	– particle diameter of $i$ -th fraction, m
$D_e$	– effective diffusivity of SO <sub>2</sub> through product layer, m <sup>2</sup> /s
$F_{Ca,CA}$	– flux of Ca in fed coal ash, kmol/s
$F_{Ca,FA}$	– flux of Ca in fly ash, kmol/s
$F_{Ca,LF}$	– flux of Ca in fine limestone particles contained in fed limestone, kmol/s
$F_{Ca,AT}$	– flux of Ca in fine limestone particles formed by attrition, kmol/s
$FC_{\text{coal}}$	– fixed carbon content of coal, kg <sub>fixed carbon</sub> /kg <sub>coal</sub> , dry basis
$G_{\text{coal}}$	– coal feed rate, kg <sub>dry coal</sub> /s
$M$	– molecular weight of CaCO <sub>3</sub> , kg/kmol
$q_S$	– specific reaction rate SO <sub>2</sub> capture rate per unit surface area, kmol/m <sup>2</sup> s
$r_S$	– SO <sub>2</sub> capture rate per unit surface area for the simplified model, kmol/m <sup>2</sup> s
$R_F$	– SO <sub>2</sub> formation rate from char particles per unit mass of bed material, kmol/kg·s
$R_S$	– SO <sub>2</sub> capture rate per unit mass of bed material, kmol/kg·s
$s_{\text{coal}}$	– sulfur content of coal, kmol <sub>sulfur</sub> /kg <sub>dry coal</sub>
$t$	– time, s
$V_G$	– volumetric gas flow rate, m <sup>3</sup> /s

$VM_{\text{coal}}$	– volatile matter content of coal, $\text{kg}_{\text{volatile matter}}/\text{kg}_{\text{coal}}$ , dry basis
$w_i$	– weight fraction of bed material that has the size of $D_{pi}$
$W_{BM}$	– mass of bed material, kg
$X_c$	– distance from the initial particle surface to unreacted core surface defined in fig. 6, m
$X_e$	– distance from the initial particle surface to the particle surface after attrition defined in fig. 6, m
$Y$	– total $\text{SO}_2$ capture rate within the reactor, kmol/s

#### Greek letters

$\alpha$	– attrition rate (rate of decrease in radius) of limestone, m/s
$\delta$	– product layer thickness, m
$\eta$	– molar fraction of $\text{CaSO}_4$ in fine limestone formed by attrition
$\eta_{\text{exper}}$	– experimentally obtained (total $\text{SO}_2$ capture rate)/(formation rate of Ca fine by attrition)
$\rho$	– density of limestone, $\text{kg}/\text{m}^3$
$\tau$	– period of attrition, s

#### References

- 1 Snow, M. J. H., Longwell, J. P., Sarofim, A. F., Direct Sulfation of Calcium Carbonate, *Ind. Eng. Chem. Res.*, 27 (1988), 2, pp. 268-273
- 2 Hajaligol, M. R., Longwell, J. P., Sarofim, A. F., Analysis and Modeling of the Direct Sulfation of  $\text{CaCO}_3$ , *Ind. Eng. Chem. Res.*, 27 (1988), 12, pp. 2203-2210
- 3 Iisa, K., Hupa, M., Rate-Limiting Processes for the Desulphurisation Reaction at Elevated Pressures, *J. Inst. Energy*, 65 (1992), 4, pp. 201-205
- 4 Krishnan, S.V., Sotirchos, S.V., Sulfation of High Purity Limestone under Simulated PFBC Conditions, *Canadian J. Chem. Eng.*, 71 (1993), 2, pp. 244-255
- 5 Krishnan, S.V., Sotirchos, S.V., A Variable Diffusivity Shrinking-Core Model and its Application to the Direct Sulfation of Limestone, *Canadian J. Chem. Eng.*, 71 (1993), 5, pp. 734-745
- 6 Zevenhoven, R., Yrjas, P., Hupa, M., Sulfur Dioxide Capture under PFBC Conditions: the Influence of Sorbent Particle Structure, *Fuel*, 77 (1998), 4, pp. 285-292
- 7 Qui, K., Lindqvist, O., Direct Sulfation of Limestone at Elevated Pressures, *Chem. Eng. Sci.*, 55 (2000), 16, pp. 3091-3100
- 8 Sakuno, S., Shimizu, T., Misawa, N., Suzuki, N., Ueda, H., Sasatsu, H., Gotou, H.,  $\text{SO}_2$  Emission Control by Limestone in a 71 MW<sub>e</sub> pressurized Fluidized Bed Combustor, Part 1. Attrition and Fragmentation of Limestone (in Japanese, *Nihon-Energy-Gakkai-Shi (J. Jpn. Inst. Energy)*, 80 (2001), 8, pp. 747-757)
- 9 Shimizu, T., Peglow, M., Sakuno, S., Misawa, N., Suzuki, N., Ueda, H., Sasatsu, H., Gotou, H., Effect of Attrition on  $\text{SO}_2$  Capture by Limestone under Pressurized Fluidized Bed Combustion Conditions – Comparison between a Mathematical Model of  $\text{SO}_2$  Capture by Single Limestone Particle under Attrition Condition and  $\text{SO}_2$  Capture in a Large-scale PFBC, *Chem. Eng. Sci.*, 56 (2001), 23, pp. 6719-6728
- 10 Shimizu, T., Peglow, M., Yamagiwa, K., Tanaka, M., Sakuno, S., Misawa, N., Suzuki, N., Ueda, H., Sasatsu, H., Gotou, H., A Simplified Model of  $\text{SO}_2$  Capture by Limestone in a 71 MW<sub>e</sub> Pressurized Fluidized Bed Combustor, *Chem. Eng. Sci.*, 57 (2002), 19, pp. 4117-4128

- 11 Shimizu, T., Peglow, M., Yamagiwa, K., Tanaka, M., Comparison among Attrition-Reaction Model of SO<sub>2</sub> Capture by Uncalcined Limestone under Pressurized Fluidized Bed Combustion Conditions, *Chem. Eng. Sci.*, (in press)
- 12 Suzuki, Y., Fundamental Studies on Pressurized Fluidized Bed Combustion at NIRE (in Japanese), Seminar on Practical Use of Pressurized Fluidized Bed Combustion System December 6, 2000, Tokyo, *Soc. Chem. Engrs. Japan*, 2000, pp. 1-10
- 13 Kunii, D., Levenspiel, O., Fluidization Engineering (2<sup>nd</sup> edition), Butterworth-Heinemann, Stoneham, USA, 1991, Chapter 12

Authors' addresses:

*T. Shimizu, K. Yamagiwa, M. Tanaka,*  
Department of Chemistry & Chemical Engineering  
Niigata University  
2-8050 Ikarashi, Niigata, Niigata Prefecture, 950-2181, Japan  
Tel&Fax: International+81-25-262-6783

*M. Peglow*  
Otto-von-Guericke University Magdeburg  
Universitätplatz 2,  
D-39016 Magdeburg, Germany

*S. Sakuno, N. Misawa, N. Suzuki, H. Ueda, H. Sasatsu, H. Gotou*  
Electric Power Development Co., Ltd.  
1-9-88 Chigasaki,  
Chigasaki-shi, Kanagawa Prefecture, 253-0041, Japan

Corresponding author (T. Shimizu):  
E-mail: [tshimizu@eng.niigata-u.ac.jp](mailto:tshimizu@eng.niigata-u.ac.jp)